ARCHIVES OF ACOUSTICS
17, 4, 525–542 (1992)

THE ENERGY DISTRIBUTION IN THE FAR FIELD RADIATED FROM THE SEMI-INFINITE UNFLANGED CYLINDRICAL WAVE-GUIDE

A. SNAKOWSKA

Department of Theoretical Physics
Pedagogical University of Rzeszów
(35-310 Rzeszów, ul. Rejtana 16)

The theory of an arbitrary axi-symmetric Bessel mode in a circular wave-guide is reviewed and applied to the analysis of the energy distribution in the far field outside the duct. The duct is assumed to be semi-infinite and perfectly rigid, and the diffraction phenomena occurring at the open end are taken into account.

The intensity directivity function as well as the power–gain function for every mode appearing in the duct, with the diffraction parameter ka changing within the limits 0–15, has been discussed.

The formulae for the intensity directivity function were derived by applying the saddle point method to the exact expression for the acoustic velocity potential. The first and second approximations are developed and the results of computed numerical characteristics are discussed.

List of symbols

a	wave-guide radius
A_l	amplitude of l–mode
c_0	speed of sound at an ambient condition
$d_l(\vartheta)$	directivity function in the first approximation
$D_l(R, \vartheta)$	directivity function in the second approximation
$f_l(z)$	jump of potential at the wave-guide surface
$F_l(w)$	Fourier transform of $f_l(z)$
$G_l(\alpha, \vartheta)$	integrand in Eq. (6)
$I(\,)$	intensity of radiation
$H_n^{(1)}(\,)$	n order Hankel function of the first kind
$J_n(\,)$	n order Bessel function
k	wave number
ka	diffraction parameter
$K_l^{(I)}(\,)$	power directivity function defined by Wajnshtejn
l, n	Bessel mode numbers
N	index of Bessel mode producing cut-off at a fixed diffraction parameter
$p(\,)$	acoustic pressure
P_0	power radiated by a spherical wave
$P_l^{(\mathrm{inc})}$	power propagated with the l incident mode
$P_l^{(\mathrm{rad})}$	power radiated outside

R_{ln}	complex reflection coefficient
r_{ln}	power reflection coefficient
r_l	total reflection coefficient
$s^{(p)}(\,)$	pressure directivity function
$S^{(p)}(\,)$	pressure directivity function defined by Morfey
$s^{(I)}(\,)$	relative power directivity function
$S^{(I)}(\,)$	intensity directivity function defined by Eq. (18)
v	radial wave number
v_R	radial velocity
w	partial wave number
$W_l(\vartheta)$	second order contribution to directivity factor
$\Phi_l^{\mathrm{inc}}(\,)$	velocity potential of incident l mode
$\Phi_l(\,)$	velocity potential of l mode
γ_l	partial wave number of l Bessel mode
μ_l	l root of J_1
ζ_0	specific impedance of the environment
ρ_0	medium density
$\mathcal{G}(\,)$	power–gain function
$*$	complex conjugate

Other symbols used in the text are standard ones and are not listed here.

1. Introduction

Ducts, pipes and tubes in which sound propagates are called wave-guides for the reason that they carry the acoustic energy so efficiently that it does not decay according to the inverse square-distance law. These phenomena have been known for a long time, at least as long ago as when man made use of his hands as a horn to be heard at a long distance.

Some experiments showing the propagation of energy in tubes were described a hundred years ago by J. TYNDALL [1]. The observations were carried out by the famous physicist, Biot, who noticed that the lowest whispear had been heard at the other end of a 950–meter–long water pipe and that the firing of a pistol had put out the candle at the outlet.

The efficiency of transmitting sound by pipes causes sometimes an undesirable noise outside the outlet, even far away from it. The necessity often arises to damp this unwanted noise for ecological, human–health, technological or other reasons. In everyday life these problems appear in connection with road traffic and aircraft transportation, the last being the most harmful nowadays. This is why there has been so much additional interest.

For this reason too, the investigations of the distribution of acoustic energy, radiated out of the duct into the free space, is of great importance, not only theoretical but also practical.

The problem of sound propagating in the circular duct and radiating outside has been considered in a few different aspects:

– the phenomena occurring at the open end — impedance of the outlet, reflection coefficients, appearance of higher order modes in the reflected wave (WAJNSHTEJN [2]), ERIKKSON [3], LEVINE and SCHWINGER [4], SNAKOWSKA and WYRZYKOWSKI [5, 6]),

– ther acoustical properties of circular ducts with some additional geometry features like nonuniform area, certain wall thickness, finite length (ALFREDSON [7], LUNDQVIST and BOSTROM [8], HUDDE [9], ANDO [10], JOHNSTON and OGIMOTO [11, 12],

– the propagation of sound in ducts with flow (JOHNSTON and OGIMOTO [11, 12], CARIER [13], MORFEY [14], LANSING et al. [15]),

– the attenuation of sound in a duct with impedance-type boundary conditions (RAWLINS [16, 17], TESTER [18]).

In the present paper we develop the intensity directivity characteristics for any axis-symmetric Bessel mode which propagates to the open and where it is partly reflected and partly radiated outside. We consider the far field taking into account all the diffraction phenomena at the outlet. The method involved is the saddle point method called also the steepest descent method.

It is undoubtful whether the energy relations in the acoustic wave radiating outside are of great interest. Some authors working on the problem restrict their investigations to the plane wave, maintaining the opinion that the latter represents the behaviour of the system well enough. It is true as long as the diffraction parameter fulfills the condition $ka < 3.83$ (the value of the first root of the Bessel function J_1) when only the plane wave can propagate along the duct without damping. Otherwise the principal mode approximation can lead to important errors, as will be demonstrated in this paper.

In Section 2 the outline of the saddle point method is presented as well as the first and second approximation formulas for the acoustical potential. In Section 3 the intensity directivity function and the power–gain function are introduced, while Section 4 contains the results of numerical calculations and conclusions.

2. Formulation of the problem. The saddle point method approximation

Let us consider the rigid semi-infinite cylindrical wave-guide of radius "a" stretching from $z = 0$ to ∞, with the z-axis being its axis of symmetry Fig. 1.

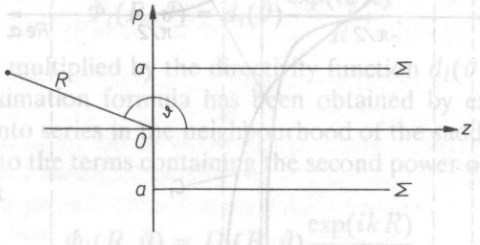

FIG. 1. Geometry of the problem.

We will only consider the axi-symmetric excitations whose time dependence is expressed by the factor $\exp(-i\omega t)$, ω being the determined frequency of vibrations. We assume that the single Bessel mode of a potential [19]

$$\Phi_l^{\text{inc}}(\rho, z) = A_l \frac{J_0(\mu_l \rho/a)}{J_0(\mu_l)} \exp(-i\gamma_l z), \tag{1}$$

where γ_l is the partial wave number related to the wave number k by the following relationship $\gamma_l = \sqrt{k^2 - \mu_l^2/a^2}$, μ_l is the l root of the Bessel function $J_1(\,)$, is incident. The wave equation solution which satisfies the hard wall boundary conditions (i.e., the

decay of the radial vibration velocity on the wave-guide wall [19]) has the form [2, 5]

$$\Phi_l(\rho, z) = \frac{ai}{4} \int_{-\infty}^{+\infty} dw \exp(iwz) v F_l(w) \begin{Bmatrix} H_0^{(1)}(v\rho) & J_1(va) \\ H_1^{(1)}(va) & J_0(v\rho) \end{Bmatrix}_{\rho<a}^{\rho>a} + \Phi_l^{\text{inc}}(\rho, z), \tag{2}$$

where w, v are partial and radial wave numbers, respectively, and $w^2 + v^2 = k^2$, $F_l(w)$ is the Fourier transform of the jump of the potential

$$f_l(z) = \Phi_l(\rho, z)|_{\rho \to a+} - \Phi_l(\rho, z)|_{\rho \to a-}. \tag{3}$$

Detailed considerations are reported in [2, 5].

The next step is to apply the saddle point method to the expression (2). The method was analysed step by step in our previous paper [20], so only an outline will be presented here.

The expression for the potential (2) is different in two partts of space $\rho > a$ and $\rho < a$, as the potential must fulfill Sommerfeld's radiation and finiteness conditions. The saddle point method must be applied to the upper and lower form of expression (2) separately.

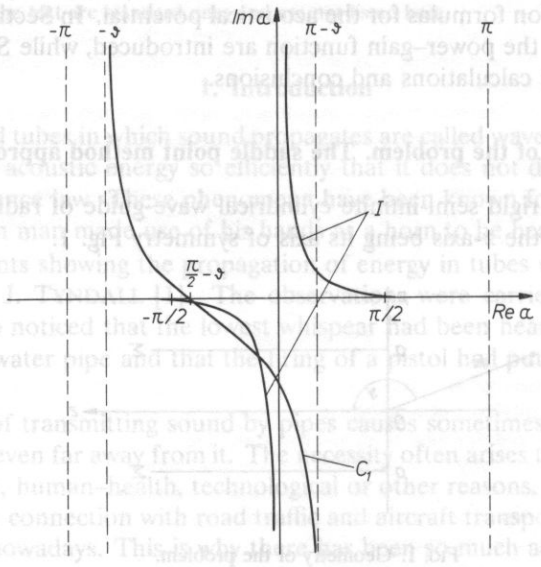

FIG. 2. Contour of integration C_1 in α complex plane.
I — cut lines of the two value function beginning at the branch points.

The saddle point method is a well known approximate method of calculating the contour integrals of the type

$$\Gamma(\Lambda) = \int G(z) \exp(\Lambda g(z))\, dz, \tag{4}$$

where $G(z)$ and $g(z)$ are analytic functions, Λ being the real parameter. To make this method applicable to our problem, we have to assume that the wave number k has a small imaginary part. This assumption allows us to consider the integrand in Eq. (2) as an analytic function and to adjust its form to the formula (3) that is, first of all, to eliminate

the exponential function. For that reason we introduce the new complex variable α as follows:

$$w = k \sin \alpha, \tag{5}$$

and apply the asymptotic form of the Hankel function $H_0^{(1)}(v\rho)$ or $J_0(v\rho)$ [21], depending on what part of space we are considering. For further calculations it will be convenient to introduce the polar coordinates (R, ϑ) so that $\rho = R \sin \vartheta$, $z = R \cos \vartheta$. After these steps we obtain the potential in the form

$$\Phi_l(R, \vartheta) = c \exp\left(\frac{i\pi}{4}\right) \int_{C_1} G_l(\alpha, \vartheta) \exp(ikR \sin(\alpha + \vartheta)) \sqrt{\cos \alpha}\, d\alpha, \tag{6}$$

the contour C_1 being plotted in Fig. 2. The explicit form of the constant c and $G_l(\alpha, \vartheta)$ for $\rho > a$ and $\rho < a$ were presented in [20]. The form of the above expression makes it possible to deduce the next step, i.e., to choose such a contour of integration which passes through the saddle point and on which the exponential function diminishes the fastest. For who has some experience in applying this method the substitution of the form

$$\sin(\alpha + \vartheta) = 1 + ix^2, \tag{7}$$

is obvious, as the exponential function in Eq. (6) takes the form $\exp(ikR) \exp(-kRx^2)$ the second term representing the function decaying exponentially with x^2. For $|kR| \gg 1$ and real k the major contribution to the integral comes from the neighbourhood of $x = 0$, which corresponds to $\alpha_0 = \pi/2 - \vartheta$.

In both parts of space $\rho > a$ and $\rho > a$ we finally obtain the same expression for the velocity potential. In the first approximation the $G_l(\alpha, \vartheta)$ function has been replaced by its value at the saddle point.

According to [20] in the first approximation we obtain the formula

$$\Phi_l(R, \vartheta) = d_l(\vartheta) \frac{\exp(ikR)}{R}, \tag{8}$$

i.e., the spherical wave multiplied by the directivity function $d_l(\vartheta)$.

The second approximation formula has been obtained by expanding the integrand $G_l(\alpha, \vartheta)$ and $\sqrt{\cos \alpha}$ into series in the neighbourhood of the saddle point and by restricting our considerations to the terms containing the second power of variable x at the most. This leads to the result

$$\Phi_l(R, \vartheta) = D_l(R, \vartheta) \frac{\exp(ikR)}{R}, \tag{9}$$

where

$$D_l(R, \vartheta) = d_l(\vartheta) + \frac{ia}{2R} W_l(\vartheta), \tag{10}$$

so in the expression for the directivity function the term depending on the distance R appears. Its contribution to the field potential decreases with the distance R, but for some values of R neglecting this term would affect the results considerably, what will be shown in the next section. It is clear that we can obtain the first approximation in the limit $R \to \infty$, so it is also called the "infinite distance approximation". Because of the rather complicated form of expressions for the above introduced quantities $F_l(w)$, $d_l(\vartheta)$, $D_l(R, \vartheta)$, we do not present their explicit forms in this paper. Readers are referred to our previous paper [20] containing all the details.

We should not forget about the limits applicability of the presented method. For the real wave number k, the results obtained are valid for $kR\sin^2\vartheta \gg 1$, this condition occurring as a result of applying asymptotic formulas.

3. Evaluation of physical quantities. Power directivity and power–gain function

Among many physical quantities useful in analysing the problem of acoustic far field outside the pipe, the pressure directivity, the power directivity, and the power–gain functions should be listed.

The pressure directivity function can be defined as a ratio of the pressure in the given direction (ϑ, φ) and the pressure of an isotropically radiating point source of equal power output:

$$s^{(p)}(R, \vartheta, \varphi) = |\Phi(R, \vartheta, \varphi)|R. \tag{11}$$

JOHNSTON and OGIMOTO [12] define the pressure directivity as

$$S^{(p)}(R, \vartheta, \varphi) = \frac{|p(R, \vartheta, \varphi)|R}{\rho_0 c_0}, \tag{12}$$

so using the well-known dependence between the velocity potential and acoustic pressure it is easy to notice that

$$S^{(p)}(R, \vartheta, \varphi) = ks^{(p)}(R, \vartheta, \varphi). \tag{13}$$

For the potential given by the formulas (8) or (9) the pressure directivity function (11) is equal to $|d_l(\vartheta)|$ and $|D_l(\vartheta)|$, respectively, the index l referring to a number of Bessel mode propagating along the pipe and radiating outside. This quantity has been considered for the diffraction parameter ka changing within the limits of (0–15), so now we will concentrate on the quantities connected with energy distribution in the far field.

WAJNSHTEJN [2] defines the power directivity function as the power radiated into a unit solid angle in the direction connected with the velocity potential in the way

$$K^{(I)}(\vartheta, \varphi) = \frac{1}{2}\rho_0 c_0 k^2 |\Phi|^2 R^2. \tag{14}$$

It is easy to find out that the above is valid only in the infinite distance approximation $R \to \infty$. As $P_0 = 1/2\rho_0 c_0 k^2$ is the power radiated into a unit solid angle by a spherical wave of a potential $\Phi = (1/R)\exp(ikR)$, we can write the last expression in the form

$$K^{(I)}(R, \vartheta, \varphi) = P_0 |\Phi|^2 R^2, \tag{15}$$

and define the related power directivity function

$$s^{(I)}(R, \vartheta, \varphi) = \frac{K^{(I)}(R, \vartheta, \varphi)}{P_0} \tag{16}$$

According to that definition, in the case of axis symmetric excitation, we obtain in the first approximation as follows:

$$s_l^{(I)}(\vartheta) = |d_l(\vartheta)|^2. \tag{17}$$

MORFEY in his work [14] introduced the intensity directivity function, applied later by JOHNSTON and OGIMOTO [12]

$$S^{(I)}(R, \vartheta, \varphi) = \rho_0 c_0 I(R, \vartheta, \varphi) R^2, \tag{18}$$

where $I(R, \vartheta, \varphi)$ is the power radiated into the unit solid angle in the direction (ϑ, φ)

$$I(R, \vartheta, \varphi) = \langle p(R, \vartheta, \varphi) v_R^*(R, \vartheta, \varphi) \rangle_t, \tag{19}$$

v_R being the radial velocity and $\langle\ \rangle_t$ denoting the time average of bracketed quantity. In the first approximation, in accordance with Eq. (8) and pressure and velocity definitions, we obtain for the l — Bessel mode propagating to the open end

$$I_l(\vartheta, \varphi) = \frac{1}{2} \rho_0 c_0 k^2 |\Phi_l|^2, \tag{20}$$

and

$$S_l^{(I)}(R, \vartheta, \varphi) = \frac{1}{2} (\rho_0 c_0 k)^2 |\Phi_l|^2 R^2, \tag{21}$$

so comparing the last expression with the one proposed by WAJNSHTEJN [14] we see that

$$S_l^{(I)}(R, \vartheta, \varphi) = \zeta_0 K_l^{(I)}(R, \vartheta, \varphi), \tag{22}$$

$\zeta_0 = \rho_0 c_0$, being the specific impedance of the environment.

We extend Wajnshtejn's definition so that it should be adequate not only in the $kR \to \infty$ approximation, writing simply that

$$K_l^{(I)}(R, \vartheta, \varphi) = I(R, \vartheta, \varphi) R^2 \tag{23}$$

In the second approximation the intensity calculated according to Eq. (9) is equal to

$$I_l(R, \vartheta) = \left\langle k^2 \rho_0 c_0 D_l(R, \vartheta) \left[D_l(R, \vartheta) + \frac{i}{R} d_l(\vartheta) \right]^* \right\rangle_l \tag{24}$$

what gives the following intensity directivity formula:

$$S_l^{(I)}(R, \vartheta) = \frac{1}{2} (k \rho_0 c_0)^2 D_l(R, \vartheta) \left[D_l(R, \vartheta) + \frac{i}{R} d_l(\vartheta) \right]^*. \tag{25}$$

It is easy to notice that the last expression differs from the one we would have obtained using Wajnshtejn's formula (14) which would be proportional to $|D_l(R, \vartheta)|^2$. The difference appears as a consequence of the phase-shift between the pressure and velocity, the difference disappearing as the distance $R \to \infty$. The Wajnshtejn definition is valid only in the infinite distance approximation, otherwise we use the formula for the potential (9), in which the directivity coefficient $D_l(R, \vartheta)$ depends on the distance R neglecting at the same time the phase-shift between pressure and velocity.

After these remarks we can extend the definition of $s_l^{(I)}(\vartheta)$ for the points in finite distance from the outlet writing

$$s_l^{(I)}(R, \vartheta) = D_l(R, \vartheta) \left[D_l(R, \vartheta) + \frac{i}{R} d_l(\vartheta) \right]^*. \tag{26}$$

It is useful to compare the power radiated outside with the power transmitted by the incident l Bessel mode. To calculate these quantities we will remind the formula for the potential inside the pipe [2, 21]:

$$\Phi_l(\rho, z) = A_l \frac{J_0(\mu_l \rho / a)}{J_0(\mu_l)} \exp(-i\gamma_l z) + \sum_{n=0}^{N} R_{ln} A_l \frac{J_0(\mu_n \rho / a)}{J_0(\mu_n)} \exp(i\gamma_n z), \tag{27}$$

where R_{ln} is the complex reflection coefficient being the ratio of the complex amplitude of the n Bessel mode which appears in the duct due to diffraction and the amplitude l of the incident l mode, N is the index of the highest mode which can propagate without damping along the duct at a fixed diffraction parameter $ka(\mu_N < ka \leq \mu_{N+1})$. That lets us calculate the power propagated with the incident mode [2, 19]

$$P_l^{\text{inc}} = \frac{1}{2}\pi a^2 \rho_0 c_0 k \gamma_l |A_l|^2, \tag{28}$$

where πa^2 is the outlet surface.

Another quantity to be discussed is the power radiated outside [2].

$$P_l^{\text{rad}} = P_l^{\text{inc}}\left[1 - \left(\sum_{n=0}^{N} |R_{ln}|^2 \frac{\gamma_n}{\gamma_l}\right)\right], \tag{29}$$

the expression under the sum sign representing the residue part of energy in the wave guide.

Introducing the power reflection coefficient as

$$r_{ln} = |R_{ln}|^2 \frac{\gamma_n}{\gamma_l}, \tag{30}$$

and total reflection coefficient as

$$r_l = \sum_{n=0}^{N} r_{ln}, \tag{31}$$

we can express the power radiated from the pipe outlet [2] as

$$P_l^{\text{rad}} = P_l^{\text{inc}}(1 - r_l). \tag{32}$$

The power directivity function integrated over the total solid angle should be equal to the quantity of power radiated outside:

$$\int_0^{2\pi} d\varphi \int_0^{\pi} K_l^{(I)}(\vartheta, \varphi) \sin\vartheta \, d\vartheta = P_l^{\text{rad}}, \tag{33}$$

so, having in mind the axis-symmetric excitation, we obtain

$$2\pi \int_0^{\pi} K_l^{(I)}(\vartheta) \sin\vartheta \, d\vartheta = P_l^{\text{rad}}. \tag{34}$$

The quantity

$$\mathcal{G}(\vartheta) = \frac{K_l^{(I)}(\vartheta)}{P_l^{\text{rad}}/4\pi}, \tag{35}$$

called the power-gain function indicates what part of outside radiated energy has been shaped in a unit solid angle and it is obvious that

$$\int_0^{\pi} \mathcal{G}(\vartheta) \sin\vartheta \, d\vartheta = 2. \tag{36}$$

4. Results of numerical calculations. Conclusions

In the previous Section some of the features of the considered quantities have been presented theoretically. The results obtained allowed doctor J. Jurkiewicz from the Noise-Lab to derive the numerical programme to calculate the intensity directivity function and the power–gain function and to analyse the results obtained with dependence on the mode number, diffraction parameter and the distance from the output.

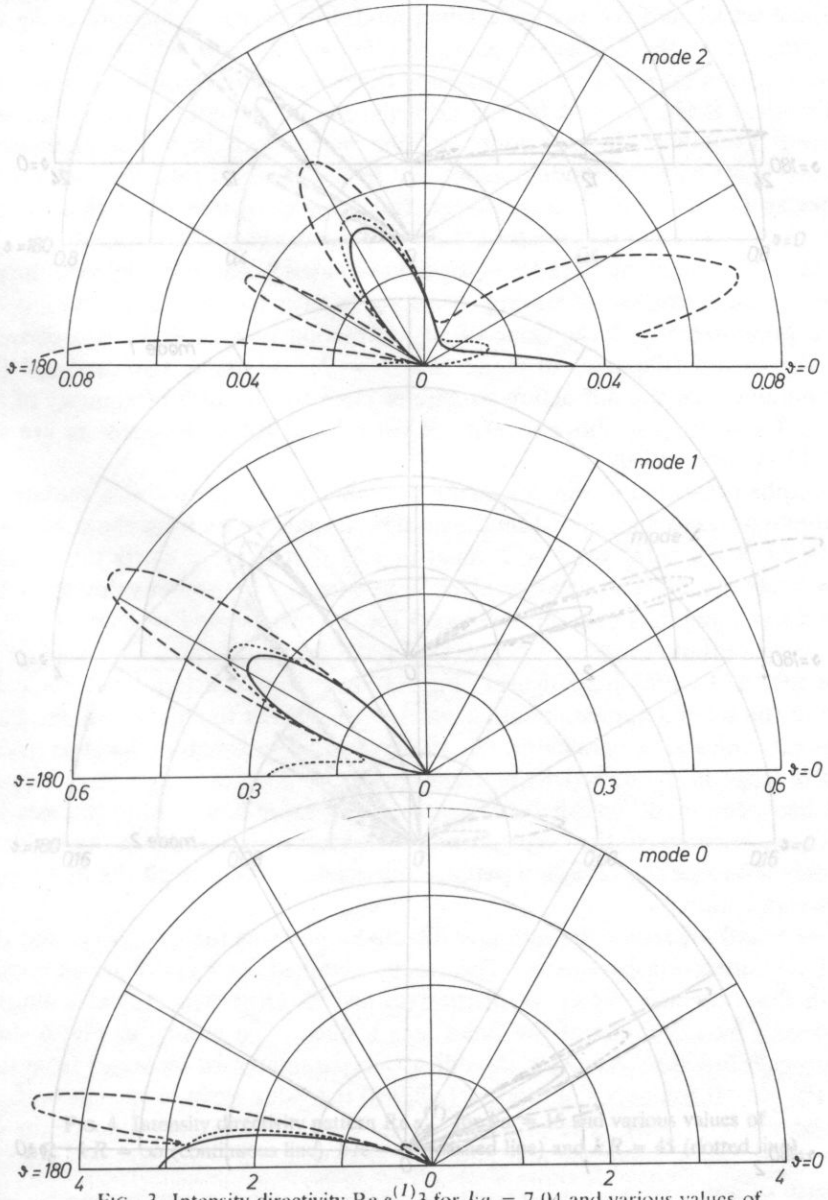

FIG. 3. Intensity directivity Re $s_i^{(1)}$ for $ka = 7.04$ and various values of kR : $kR = \infty$ (continuous line), $kR = 7$ (dashed line) and $kR = 21$ (dotted line).

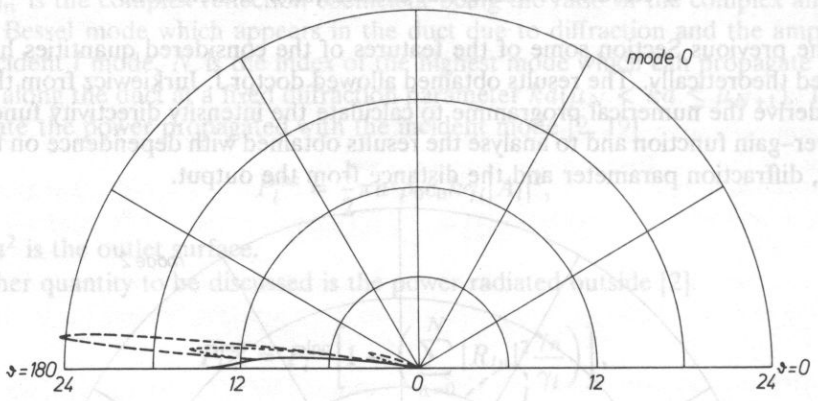
mode 0
ϑ=180
24
12
0
12
24
ϑ=0

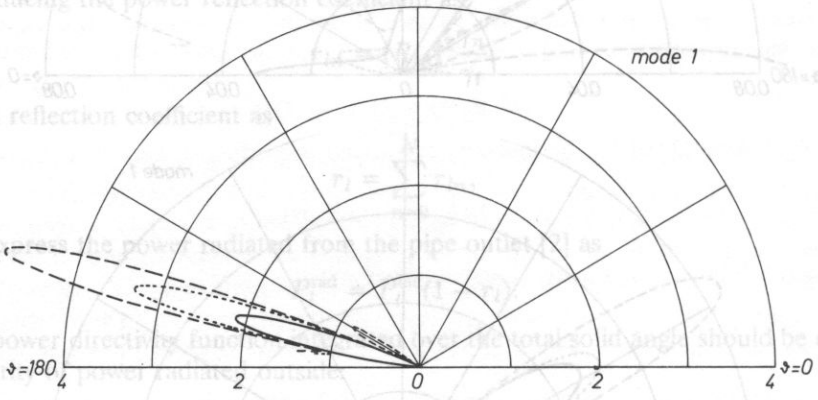
mode 1
ϑ=180
4
2
0
2
4
ϑ=0

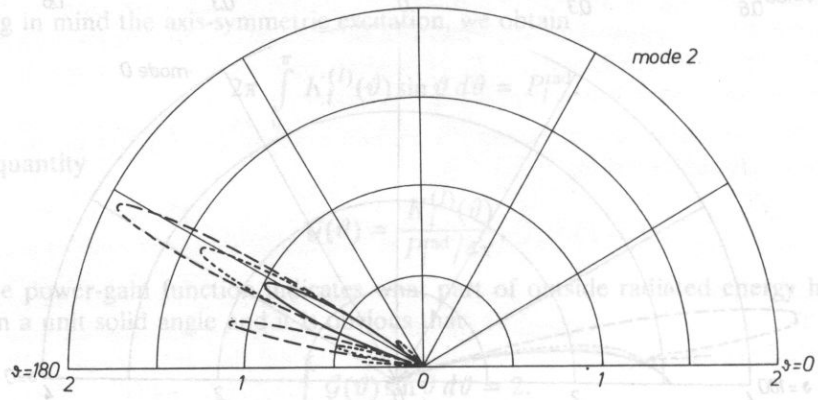
mode 2
ϑ=180
2
1
0
1
2
ϑ=0

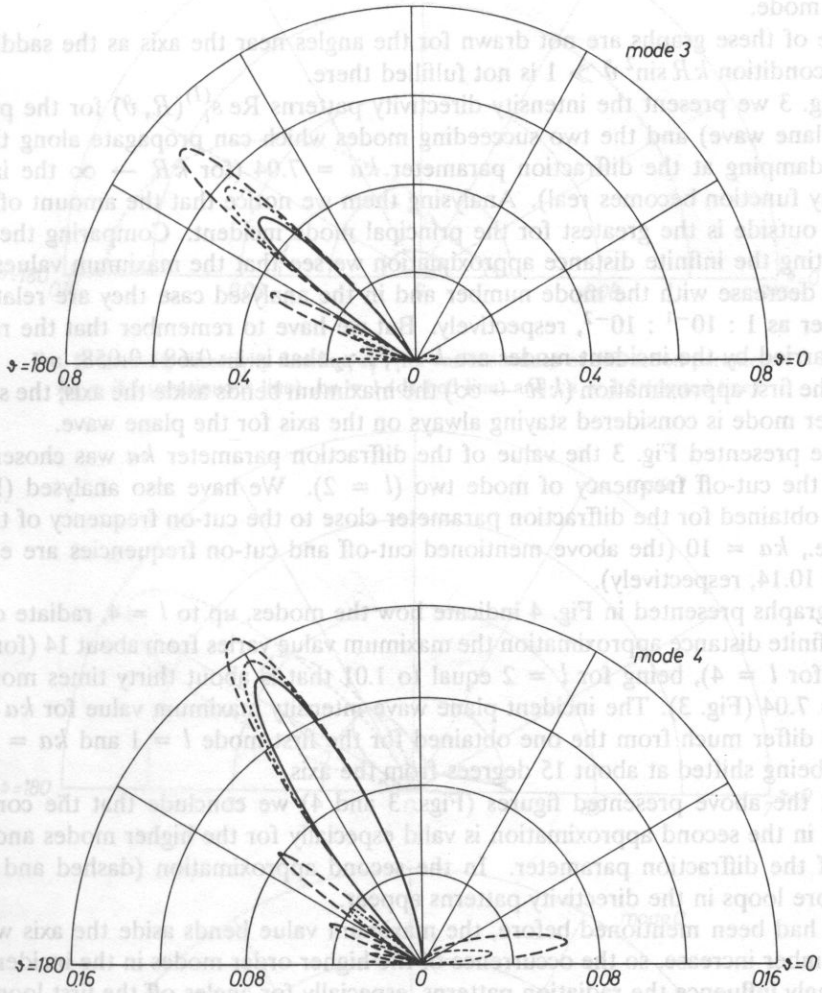

FIG. 4. Intensity directivity pattern $\mathrm{Re}\, s_1^{(I)}$ for $ka = 15$ and various values of kR : $kR = \infty$ (continuous line), $kR = 30$ (dashed line) and $kR = 45$ (dotted line).

The assumption was made that the single Bessel mode allowed for the fixed diffraction parameter, propagates towards the open end. The diffraction phenomena at the output was taken into account. In all the considered cases we assumed the unit amplitude of the incident mode.

Some of these graphs are not drawn for the angles near the axis as the saddle-point method condition $kR\sin^2\vartheta \gg 1$ is not fulfilled there.

In Fig. 3 we present the intensity directivity patterns $\mathrm{Re}\, s_l^{(I)}(R,\vartheta)$ for the principal mode (plane wave) and the two succeeding modes which can propagate along the duct without damping at the diffraction parameter $ka = 7.04$ (for $kR \to \infty$ the intensity directivity function becomes real). Analysing them we notice that the amount of energy radiated outside is the greatest for the principal mode incident. Comparing the graphs representing the infinite distance approximation we see that the maximum values of the intensity decrease with the mode number and in the analysed case they are related one to another as $1 : 10^{-1} : 10^{-2}$, respectively. But we have to remember that the ratios of energy carried by the incident modes are $k : \gamma_1 : \gamma_2$ that is $1 : 0.68 : 0.058$.

For the first approximation ($kR \to \infty$) the maximum bends aside the axis, the stronger the higher mode is considered staying always on the axis for the plane wave.

In the presented Fig. 3 the value of the diffraction parameter ka was chosen to be close to the cut-off frequency of mode two ($l = 2$). We have also analysed (Fig. 4) the date obtained for the diffraction parameter close to the cut-on frequency of the next mode, i.e., $ka = 10$ (the above mentioned cut-off and cut-on frequencies are equal to 7.02 and 10.14, respectively).

The graphs presented in Fig. 4 indicate how the modes, up to $l = 4$, radiate outside. In the infinite distance approximation the maximum value varies from about 14 (for $l = 0$) to 0.14 (for $l = 4$), being for $l = 2$ equal to 1.01 that is about thirty times more than for $ka = 7.04$ (Fig. 3). The incident plane wave intensity maximum value for $ka = 7.04$ does not differ much from the one obtained for the first mode $l = 1$ and $ka = 15$, the last one being shifted at about 15 degrees from the axis.

From the above presented figures (Figs. 3 and 4) we conclude that the correction obtained in the second approximation is valid especially for the higher modes and larger values of the diffraction parameter. In the second approximation (dashed and dotted lines) more loops in the directivity patterns appear.

As it had been mentioned before, the maximum value bends aside the axis with the mode number increase, so the occurrence of the higher order modes in the incident wave can strongly influence the radiation patterns, especially for angles off the first loop of the plane wave radiation.

Figures 5 and 6 present the intensity directivity patterns for $kR \to \infty$ and different values of the diffraction parameter. The results obtained for $ka = 1$ are in good agreement with these obtained by G. W. JOHNSTON and K. OGIMOTO [12] as a limiting case in considering radiation out of the finite length duct. The graphs in Fig. 6 show how the power–gain function changes if the diffraction parameter ka increases from the value close to the cut-off frequency of mode 1 (3.83) to the value close to the cut-on frequency of the next mode (7.016). The principal mode has always its maximum in the forward direction ($\vartheta = 180°$), while the maximum of the first mode bends towards the axis with the increase of ka.

In the next two figures (Figs. 7 and 8) we present the power–gain function for different

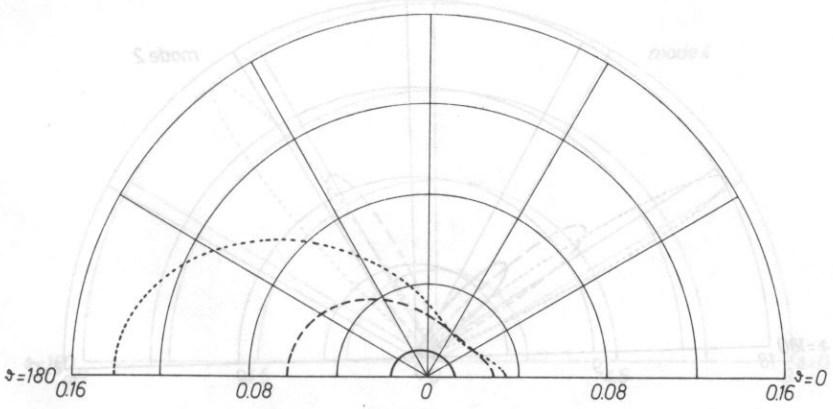

FIG. 5. Intensity directivity function $s_l^{(I)}$ for various values of diffraction parameter: $ka = 0.5$ (continuous line), $ka = 1$ (dashed line) and $ka = 1.5$ (dotted line).

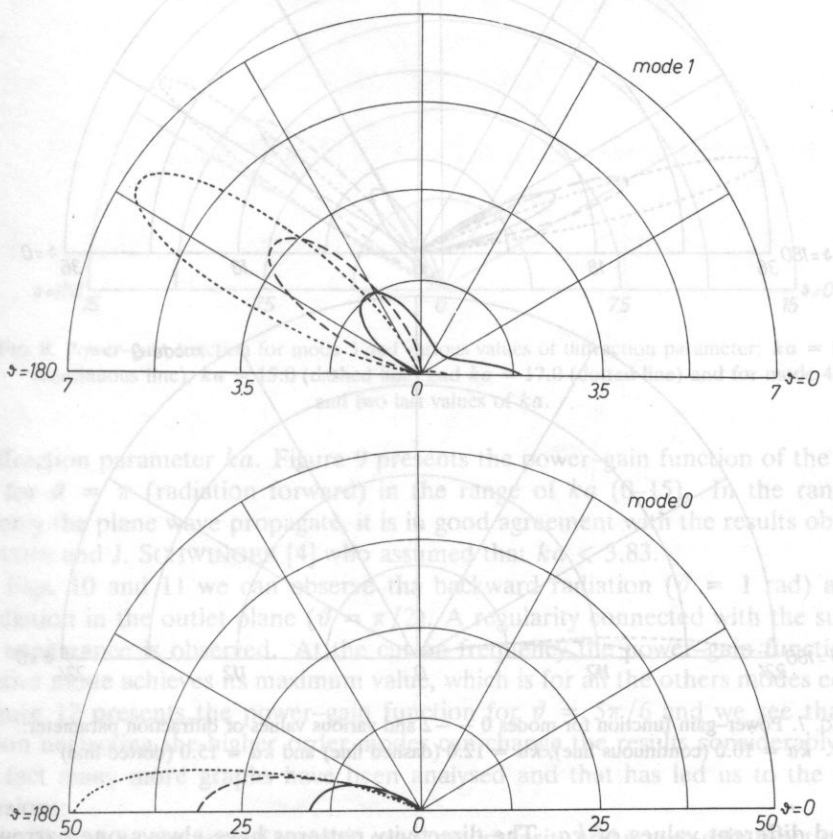

FIG. 6. Power–gain function for modes 0–2 and various values of diffraction parameter: $ka = 3.85$ (continuos line), $ka = 5.5$ (dashed line) and $ka = 7.0$ (dotted line).

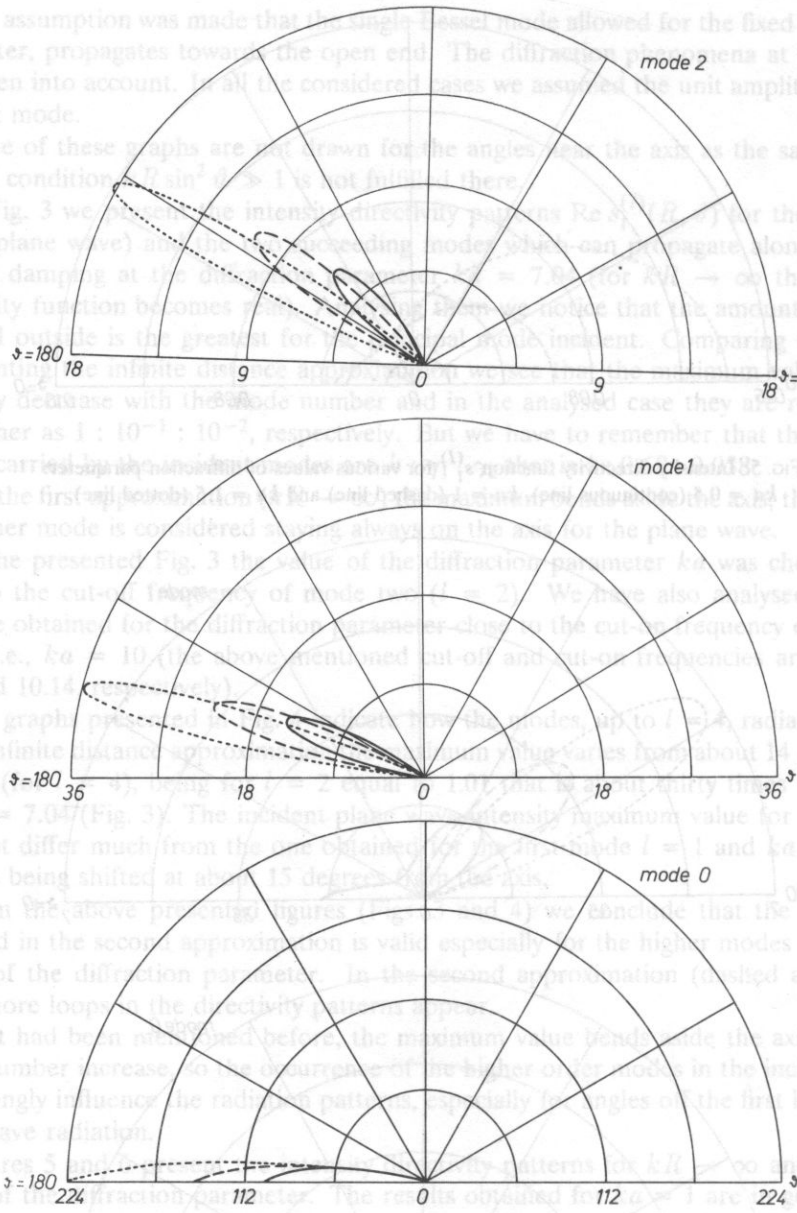

FIG. 7. Power–gain function for modes $0 - -2$ and various values of diffraction parameter: $ka = 10.0$ (continuous line), $ka = 12.0$ (dashed line) and $ka = 15.0$ (dotted line)

modes and different values of ka. The directivity patterns have always one narrow loop which shifts from the axis with the mode number increase, but for the same mode ($n = 0$) its maximum bends towards the axis for larger ka.

The next figures show how the power–gain function of the fixed angle changes with

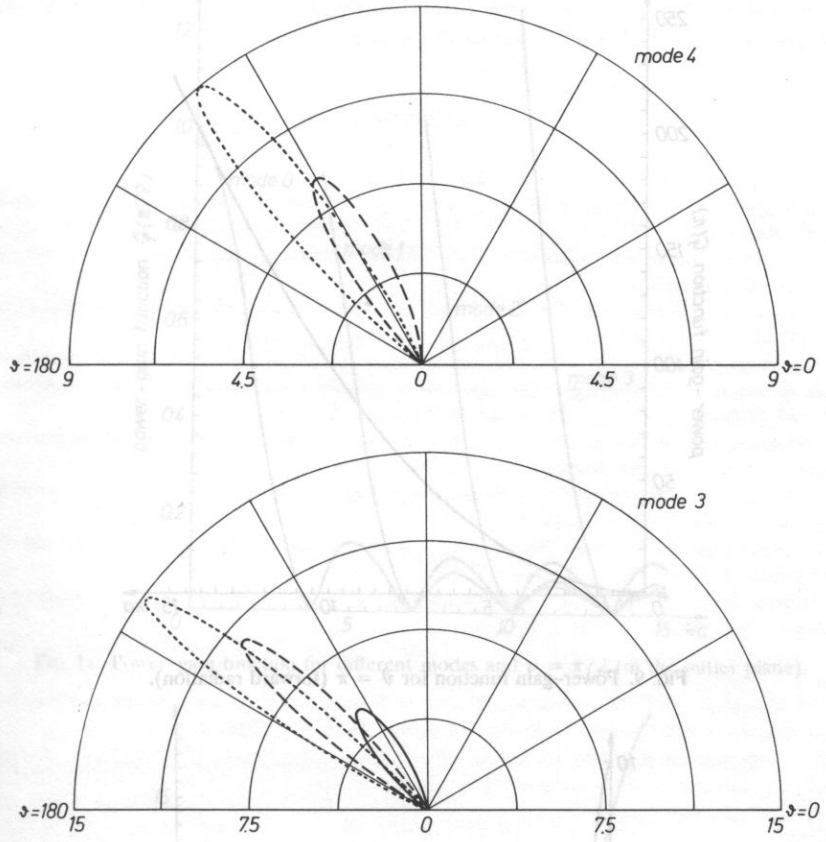

FIG. 8. Power–gain function for mode 3 and various values of diffraction parameter: $ka = 12.0$ (continuous line), $ka = 15.0$ (dashed line) and $ka = 17.0$ (dotted line) and for mode 4 and two last values of ka.

the diffraction parameter ka. Figure 9 presents the power–gain function of the principal mode for $\vartheta = \pi$ (radiation forward) in the range of ka (0–15). In the range of ka when only the plane wave propagate, it is in good agreement with the results obtained by H. LEVINE and J. SCHWINGER [4] who assumed that $ka < 3.83$.

In Figs. 10 and 11 we can observe tha backward radiation ($\vartheta = 1$ rad) as well as the radiation in the outlet plane ($\vartheta = \pi/2$). A regularity connected with the succeeding mode appearance is observed. At the cut-on frequency the power–gain function of the respective mode achieves its maximum value, which is for all the others modes equal to 0.

Figure 12 presents the power–gain function for $\vartheta = 5\pi/6$ and we see that in that direction neglecting the higher order modes can change the results considerably.

In fact many more graphs have been analysed and that has led us to the following conclusions:

– the directivity patterns of acoustic pressure, intensity and power-gain function depend strongly on the number of the Bessel mode incident

– the maximum values bend aside the axis with the mode number increase

– the correction obtained in the second approximation is valid especially for the higher

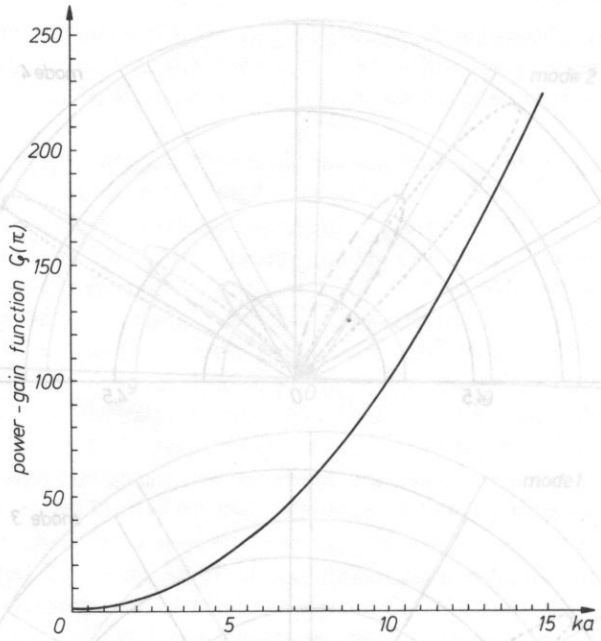

FIG. 9. Power–gain function for $\vartheta = \pi$ (forward radiation).

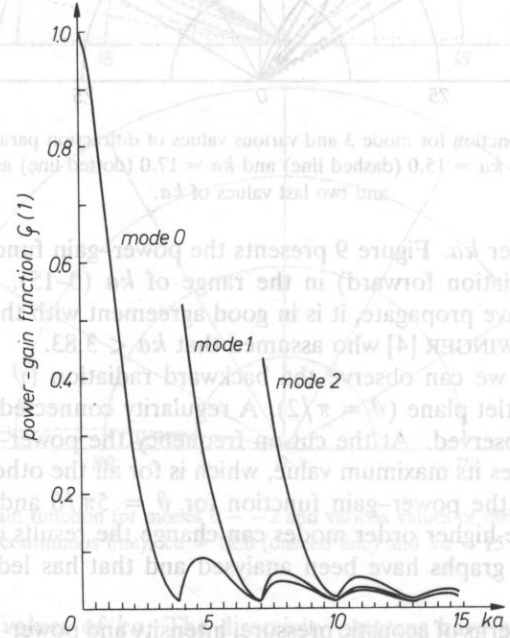

FIG. 10. Power–gain function for different modes and $\vartheta = 1$ (backward radiation).

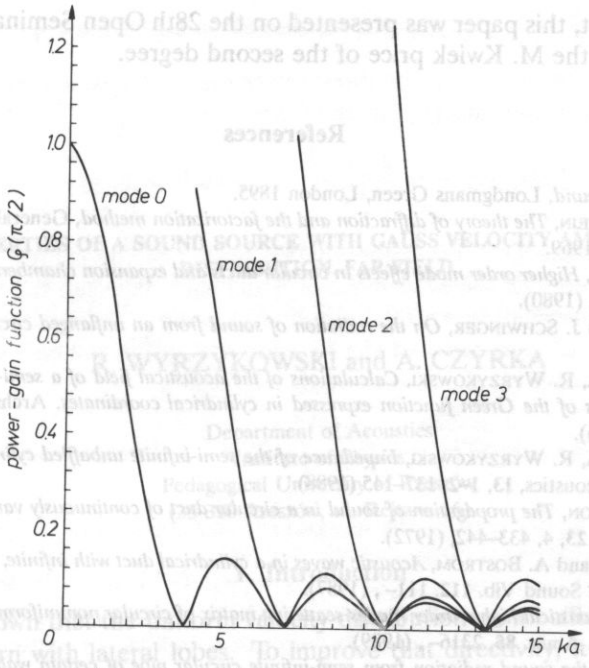

FIG. 11. Power–gain function for different modes and $\vartheta = \pi/2$ (in the outer plane).

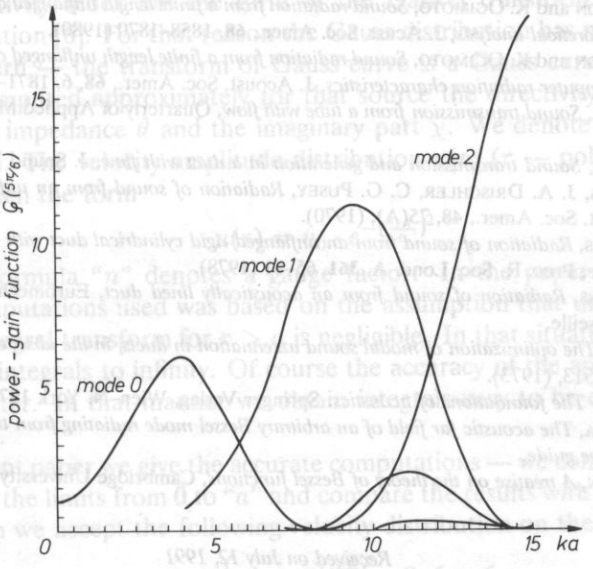

FIG. 12. Power–gain function for different modes and $\vartheta = 5\pi/6$.

modes and larger values of the diffraction parameter

– a regularity connected with the succeeding mode appearance is observed.

From the above presented results it is undoubtful that in many analyses of the energy distribution the plane wave approximation can yield significant errors.

To some extent, this paper was presented on the 28th Open Seminar on Acoustics and was honoured by the M. Kwiek price of the second degree.

References

[1] J. TYNDALL, *Sound*, Londgmans Green, London 1895.

[2] L. A. WAJNSHTEJN, *The theory of diffraction and the factorization method*, Generalized Wiener-Hopf technique, Golem 1969.

[3] L. J. ERIKKSON, *Higher order mode effects in circular ducts and expansion chambers*, J. Acoust. Soc. Amer., **68**, 2, 545–550, (1980).

[4] H. LEVINE and J. SCHWINGER, *On the radiation of sound from an unflanged circular pipe*, Phys. Rev. **73**, 383- (1948).

[5] A. SNAKOWSKA, R. WYRZYKOWSKI, *Calculations of the acoustical field of a semi-infinite cylindrical waveguide by means of the Green function expressed in cylindrical coordinates*. Archives of Acoustics, **11**, 3, 261–285, (1986).

[6] A. SNAKOWSKA, R. WYRZYKOWSKI, *Impedance of the semi-infinite unbaffled cylindrical wave-guide outlet*, Archives of Acoustics, **13**, 1–2, 137–145 (1988).

[7] R. J. ALFREDSON, *The propagation of sound in a circular duct of continuously varying cross-sectional area*, J. Sound Vib., **23**, 4, 433–442, (1972).

[8] L. LUNDOVIST and A. BOSTRÖM, *Acoustic waves in a cylindrical duct with infinite, half-infinite or finite wall corrugations*, J. Sound Vib. **112**, 111– , (1987).

[9] H. HUDDE, *Acoustical higher-order modes scattering matrix of circular nonuniform lossy tubes without flow*, J. Acoust. Soc. Amer. **85**, 2316– , (1989).

[10] Y. ANDO, *On the sound radiation from semi-infinite circular pipe of certain wall thickness*. Acustica, **22**, 219–225, (1969).

[11] G. W. JOHNSTON and K. OGIMOTO, *Sound radiation from a finite length unflanged circular duct with uniform axial flow. Theoretical analysis*, J. Acust. Soc. Amer., **68**, 1858–1870 (1980).

[12] G. W. JOHNSTON and K. OGIMOTO, *Sound radiation from a finite length unflanged circular duct with uniform axial flow. Computer radiation characteristics*, J. Acoust. Soc. Amer., **68**, 6, 1871–1883 (1980).

[13] G. F. CARRIER, *Sound transmission from a tube with flow*, Quarterly of Applied Mathematics, **13**, 453–461, (1956).

[14] C. L. MORFEY, *Sound transmission and generation in a duct with flow*, J. Sound Vib., **14**, 37–55, (1971).

[15] D. L. LANSING, J. A. DRISCHLER, C. G. PUSEY, *Radiation of sound from an unflanged circular duct with flow*, J. Acoust. Soc. Amer., **48**, 75(A), (1970).

[16] A. D. RAWLINS, *Radiation of sound from an unflanged rigid cylindrical duct with an acoustically absorbing internal surface*, Proc. R. Soc. Lond. A. **361**, 65–91 (1978).

[17] A. D. RAWLINS, *Radiation of sound from an acoustically lined duct*, Euromech 94 Conference held at C.N.R.S. Marseille.

[18] B. J. TESTER, *The optimization of modal sound azzenuation in ducts, in the absence of mean flow*, J. Sound Vib., **27**, 477–513, (1973).

[19] E. SKUDRZYK, *The foundations of acoustics*. Springer-Verlag, Wien–N. York 1971.

[20] A. SNAKOWSKA, *The acoustic far field of an arbitrary Bessel mode radiating from the semi infinite unflanged cylindrical wave guide*,

[21] G. N. WATSON, *A treatise on the theory of Bessel functions*, Cambridge University Press, Cambridge, 1958.

Received on July 12, 1991